Electronic Supplementary Information

Nitrogen-rich activated carbon monoliths via ice-templating with high CO_2 and H_2 adsorption capacities

Aled D. Roberts,[a,b] Jet-Sing M. Lee,[a] Siew Yee Wong,[b] Xu Li*[b,c] and Haifei Zhang*[a]

[a] *Department of Chemistry, University of Liverpool, United Kingdom, L69 7ZD.*
[b] *Institute of Materials Research and Engineering (IMRE), 2 Fusionopolis Way, Innovis, #08-03, Singapore 138634.*
[c] *Department of Chemistry, National University of Singapore, 3 Science Drive, Singapore 117543.*
E-mail: zhanghf@liv.ac.uk(HZ), x-li@imre.a-star.edu.sg (XL).

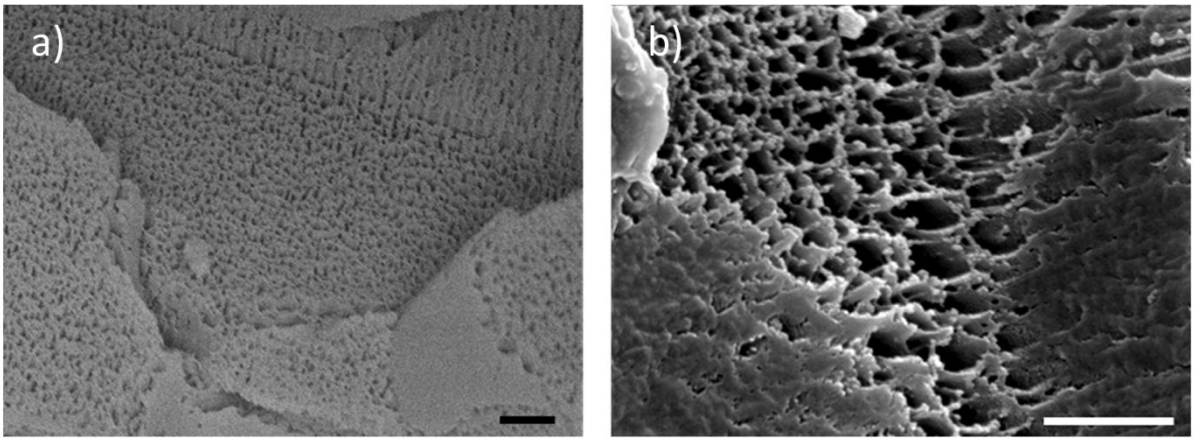

Fig. S1 SEM images of the ice-templated PAN polymer (IT-PAN10) at a) x11000 and b) x27000 magnification. Scale bar = 1 µm

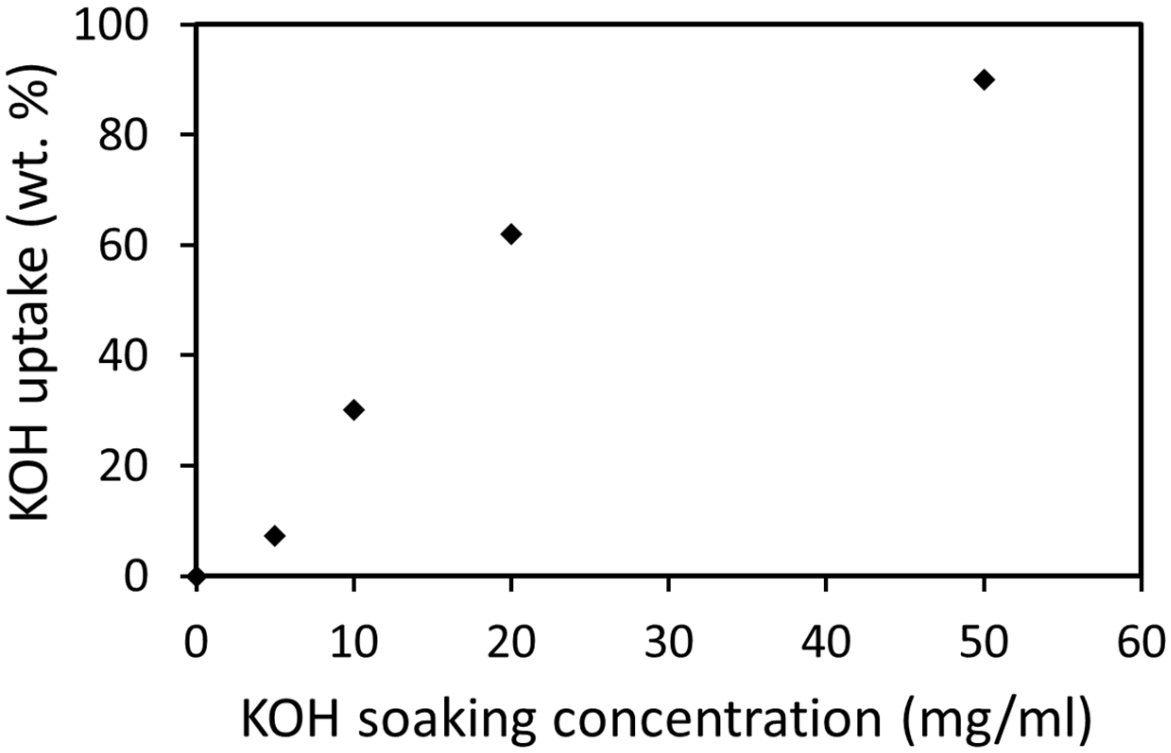

Fig. S2 Relationship between KOH soaking concentration and KOH uptake within the ice-templated porous PAN.

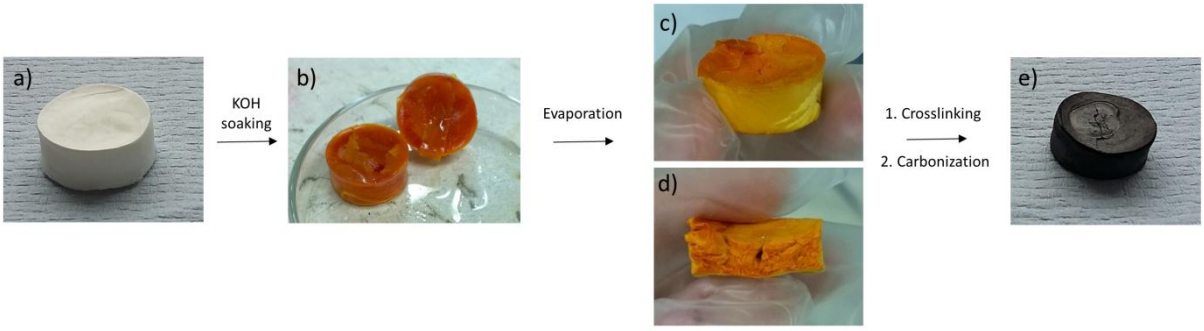

Fig. S3 a) IT-PAN10 monolith, b) after soaking in 10 mg ml^{-1} aqueous KOH, c) after KOH soaking and drying, d) cross-sectional view after KOH soaking and drying e) after crosslinking and carbonization (IT-AC10).

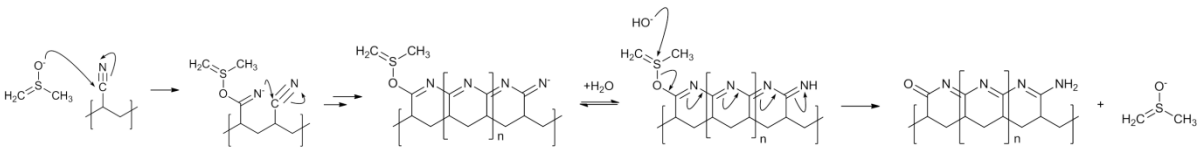

Fig. S4 Proposed base-catalysed intra-molecular cyclization of the nitrile backbone of the PAN polymer into a conjugated ladder-type polymer

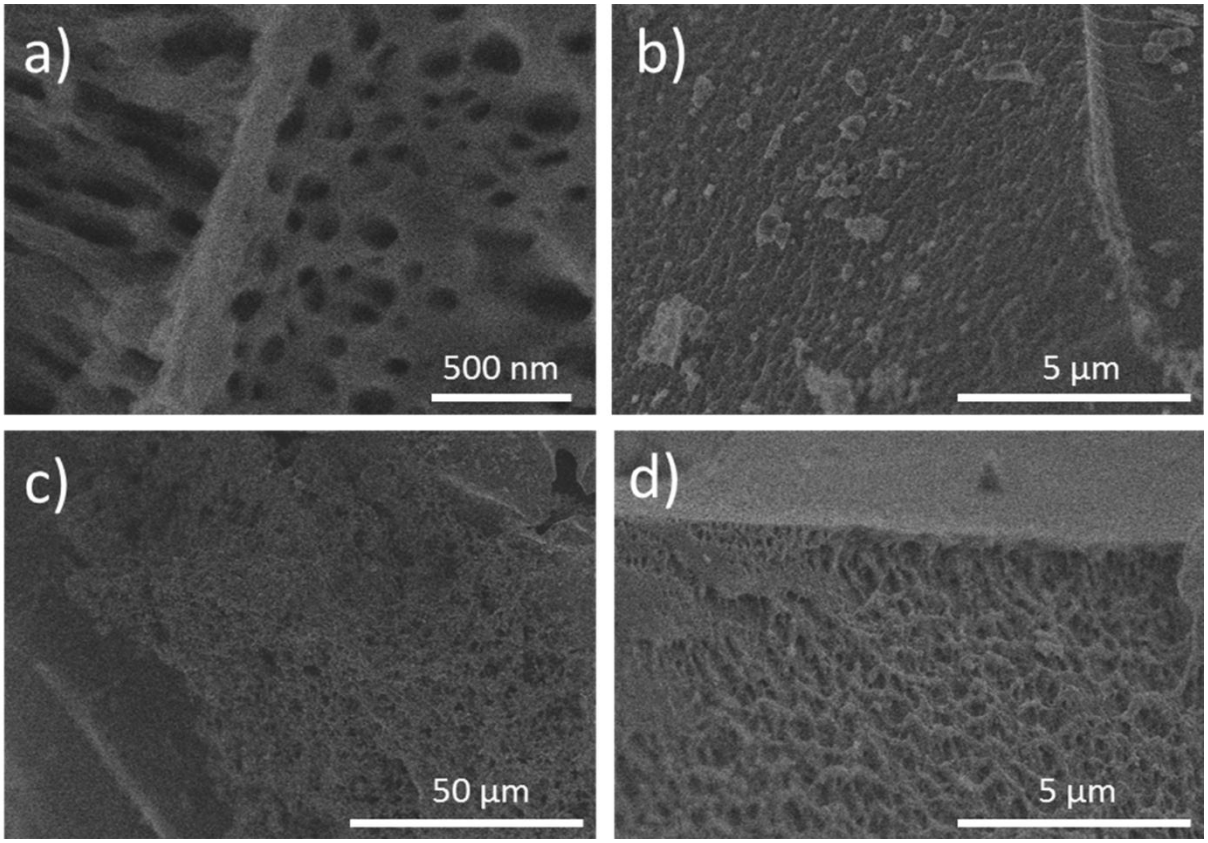

Fig. S5 SEM images of carbonized samples of ice-templated PAN: a) IT-AC5, b) IT-AC10, c) IT-AC50 and d) IT-ACMAX

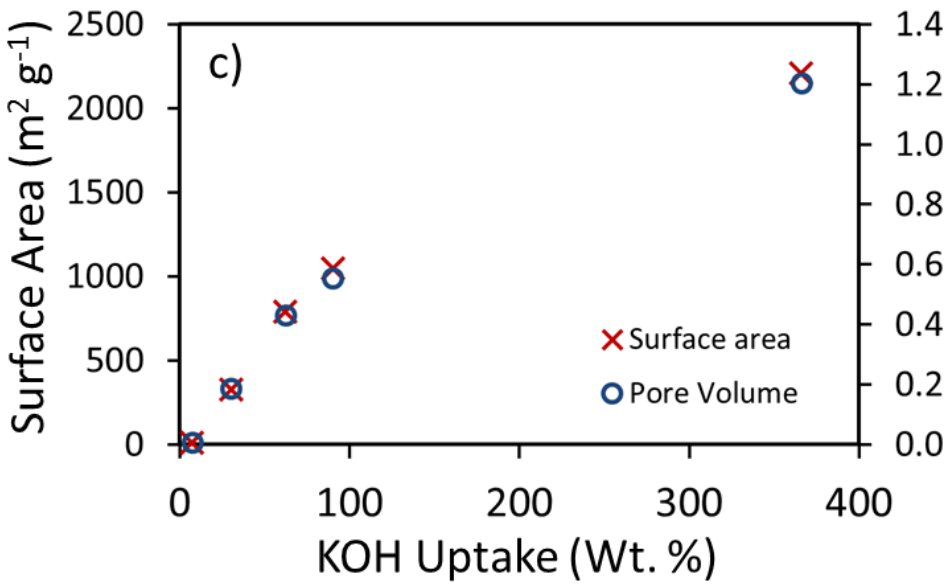

Fig. S6. The relationship of the BET surface areas for the porous activated carbon with the KOH uptake into the porous ice-templated PANs.

Table S1 CO_2 adsorption capacities of various templated carbons published in the literature

Template	Precursor	Method	BET SSA ($m^2 g^{-1}$)	N-content (wt. %)	CO_2 Adsorption (mmol g^{-1})	Conditions	Ref.
Pluronic F127	Resorcinol & Formaldehyde (RF)	RF polymerization with amine, carbonization	670	0.28	3.3	298 K, ~1 Bar	[1]
Pluronic F127	Resorcinol & Formaldehyde (RF)	RF polymerization with amine, carbonization and KOH activation	1613	0.68	3.1	298 K. 0.95 Bar	[2]
Pluronic F127	Dicyandiamide, Resol	Polymerization, carbonization	1417	6.7	3.2	298 K, 1 Bar	[3]
Pluronic 123	Polypyrrole	Polymerization of pyrrole, carbonization	941	5.8	4.5	298 K, 1 Bar	[4]
Benzimidazole-Linked Polymers	Benzimidazole-Linked Polymers	Direct carbonization (polymer acts as precursor and template) & KOH activation	1630	7.9	5.8	298 K, 1 Bar	[5]
Hypercrosslinked porous polymer (COP)	Hypercrosslinked porous polymer (COP)	Direct carbonization & KOH activation	1950	Not given	7.6	273 K, 1 Bar	[6]
Zeolite EMC-2	Acetonitrile	CVD	2559	6 - 7	4.0	298 K, ~1Bar	[7]
Zeolite EMC-2	Acetonitrile	CVD	3360	4.7	4.4	298 K, 1 Bar	[8]
ZIF-69	ZIF-69	Direct carbonization (ZIF acts as template and precursor) & KOH activation	2264	1.2	4.8	273 K, 1 Bar	[9]
MOF-5	MOF-5	Direct carbonization (MOF acts as template and precursor)	2734	Not given	27.4	300 K, 30 Bar	[10]
MOF-74	MOF-74	Direct carbonization (MOF acts as template and precursor)	2495	Not given	3.4	300 K, 1.5 Bar	[10]
Polymer microspheres (GDMA-*co*-MAA)	Melamine (ML)	ML polymerization, carbonization & KOH activation	683	14.5	2.7	298 K, 1 Bar	[11]
Mesoporous Silica (IBN-9)	Furfuryl Alcohol & p-diaminobenzene	Mixing precursors & templates, drying, carbonization & activation	890	13	10.5	298 K, 8 Bar	[12]
Mesoporous silica (SBA-15) spheres	Ethylenediamine & carbon tetrachloride	Mixing, polymerization & carbonization	550	17.8	2.9	298 K, 1 ~Bar	[13]
Sol-gel method*	Polyaniline (PANi)	PANi polymerization (hydrogel) and freeze-drying (xerogel), carbonization and KOH activation	4196	0.55	28.3	298 K, 30 Bar	[14]
Sol-gel method*	Resorcinol & Formaldehyde (RF)	RF polymerization and air-drying (aerogel), carbonization	1521	Not given	3.0	298 K, 1 Bar	[15]
Temperature induced phase separation (TIPS)*	Polyacrylonitrile (PAN)	Carbonization & CO_2 activation	2501	1.8	10.6	298 K, 3 Bar	[16]
DMSO Ice-crystals	Polyacrylonitrile (PAN)	This work (IT-AC50)	1049	14.9	16.1	298 K, 10 Bar	This Work
DMSO Ice-crystals	Polyacrylonitrile (PAN)	This work (IT-AC50)	1049	14.9	3.2	298 K ~1 Bar	This Work

* Not a templating method but included for comparison

Table S2 H_2 adsorption capacities of various templated carbons published in the literature

Template	Precursor	Method	BET SSA ($m^2 g^{-1}$)	H_2 Adsorption (wt. %)	Conditions	Ref.
Zeolite Y	Acetonitrile	CVD, post-activation w. KOH	3064	2.6	77 K, 1 Bar	[17]
Zeolite β	Acetonitrile	CVD	3150	2.6	77 K, 1 Bar	[18]
Zeolite 13X	Acetonitrile	CVD	1589	1.6	77 K, 1 Bar	[19]
Zeolite Y	Acetonitrile	CVD	1825	2.0	77K, 1 Bar	[19]
Zeolite Y	Propylene	CVD	2117	2.0	77K, 1 Bar	[20]
Mesoporous Silica (MCM-48)	Sucrose	Aqueous impregnation & carbonization	2390	3.5	77K, 1 Bar	[21]
Mesoporous Silica (MCM-48)	Sucrose	Aqueous impregnation & carbonization	1646	2.7	77K, 60 Bar	[22]
Mesoporous Silica (KIT-6)	Polycarbosilane	Organic impregnation & carbonization	2914	3.0	77 K, 135 Bar	[23]
Mesoporous Silica (SBA-15)	Sucrose	Aqueous impregnation, carbonization & CO_2 activation	2749	2.3	77 K, 1 Bar	[24]
Colloidal Silica	Sucrose	Aerosol drying & carbonization	1995	2.0	77 K, 1.1 Bar	[25]
MOF (IRMOF-1)	MOF (IRMOF-1)	Direct carbonization (MOF acts as template and precursor)	3447	3.3	77 K, 1 Bar	[26]
ZIF-8	ZIF-8	Direct carbonization (ZIF acts as template and precursor) & KOH activation	2437	2.6	77 K, ~1 Bar	[9]
Hypercrosslinked porous polymer (COP)	Hypercrosslinked porous polymer (COP)	Direct carbonization & KOH activation	2189	2.6	77 K, 1 Bar	[6]
Sol-gel method*	Resorcinol & Formaldehyde (RF)	RF polymerization and air-drying (aerogel), carbonization	1980	4.3	77 K, 20 Bar	[15]
DMSO Ice-crystals	Polyacrylonitrile (PAN)	This Work (IT-ACMAX)	2206	2.7	77 K, 1.2 Bar	This work

* Not a templating method but included for comparison

References for Table S1 and Table S2

[1] G.-P. Hao, W.-C. Li, D. Qian, G.-H. Wang, W.-P. Zhang, T. Zhang, A.-Q. Wang, F. Schüth, H.-J. Bongard, and A.-H. Lu, Structurally Designed Synthesis of Mechanically Stable Poly(benzoxazine-co-resol)-Based Porous Carbon Monoliths and Their Application as High-Performance CO_2 Capture Sorbents, *J. Am. Chem. Soc.*, 2011, **133**, 11378–11388.

[2] J. Yu, M. Guo, F. Muhammad, A. Wang, F. Zhang, Q. Li, and G. Zhu, One-pot synthesis of highly ordered nitrogen-containing mesoporous carbon with resorcinol–urea–formaldehyde resin for CO_2 capture, *Carbon,* 2014, **69**, 502–514.

[3] J. Wei, D. Zhou, Z. Sun, Y. Deng, Y. Xia, and D. Zhao, A Controllable Synthesis of Rich Nitrogen-Doped Ordered Mesoporous Carbon for CO_2 Capture and Supercapacitors, *Adv. Funct. Mater.*, 2013, **23**, 2322–2328.

[4] J. W. F. To, J. He, J. Mei, R. Haghpanah, Z. Chen, T. Kurosawa, S. Chen, W.-G. Bae, L. Pan, J. B.-H. Tok, J. Wilcox, and Z. Bao, Hierarchical N-Doped Carbon as CO_2 Adsorbent with High CO_2 Selectivity from Rationally Designed Polypyrrole Precursor, *J. Am. Chem. Soc.*, 2016, **138**, 1001–1009.

[5] B. Ashourirad, A. K. Sekizkardes, S. Altarawneh, and H. M. El-Kaderi, Exceptional Gas Adsorption Properties by Nitrogen-Doped Porous Carbons Derived from Benzimidazole-Linked Polymers, *Chem. Mater.*, 2015, **27**, 1349–1358.

[6] A. Modak and A. Bhaumik, Porous carbon derived via KOH activation of a hypercrosslinked porous organic polymer for efficient CO_2, CH_4, H_2 adsorptions and high CO_2/N_2 selectivity, *J. Solid State Chem.*, 2015, **232**, 157–162.

[7] L. Wang and R. T. Yang, Significantly Increased CO_2 Adsorption Performance of Nanostructured Templated Carbon by Tuning Surface Area and Nitrogen Doping, *J. Phys. Chem. C*, 2012, **116**, 1099–1106.

[8] Y. Xia, R. Mokaya, G. S. Walker, and Y. Zhu, Superior CO_2 Adsorption Capacity on N-doped, High-Surface-Area, Microporous Carbons Templated from Zeolite, *Adv. Energy Mater.*, 2011, **1**, 678–683.

[9] Q. Wang, W. Xia, W. Guo, L. An, D. Xia, and R. Zou, Functional Zeolitic-Imidazolate-Framework-Templated Porous Carbon Materials for CO_2 Capture and Enhanced Capacitors, *Chem. - An Asian J.*, 2013, **8**, 1879–1885.

[10] G. Srinivas, V. Krungleviciute, Z.-X. Guo, and T. Yildirim, Exceptional CO_2 capture in a hierarchically porous carbon with simultaneous high surface area and pore volume, *Energy Environ. Sci.*, 2014, **7**, 335–342.

[11] D. Li, Y. Chen, M. Zheng, H. Zhao, Y. Zhao, and Z. Sun, Hierarchically Structured Porous Nitrogen-Doped Carbon for Highly Selective CO_2 Capture, *ACS Sustain. Chem. Eng.*, 2016, **4**, 298–304.

[12] Y. Zhao, L. Zhao, K. X. Yao, Y. Yang, Q. Zhang, and Y. Han, Novel porous carbon materials with ultrahigh nitrogen contents for selective CO_2 capture, *J. Mater. Chem.*, 2012, **22**, 19726.

[13] Q. Li, J. Yang, D. Feng, Z. Wu, Q. Wu, S. S. Park, C.-S. Ha, and D. Zhao, Facile synthesis of porous carbon nitride spheres with hierarchical three-dimensional mesostructures for CO_2 capture, *Nano Res.*, 2010, **3**, 632–642.

[14] J. He, J. W. F. To, P. C. Psarras, H. Yan, T. Atkinson, R. T. Holmes, D. Nordlund, Z. Bao, and J. Wilcox, Tunable Polyaniline-Based Porous Carbon with Ultrahigh Surface Area for CO_2 Capture at Elevated Pressure, *Adv. Energy Mater.*, 2016, **6**, 1502491.

[15] C. Robertson and R. Mokaya, Microporous activated carbon aerogels via a simple subcritical drying route for CO_2 capture and hydrogen storage, *Micropor. Mesopor.Mater.*, 2013, **179**, 151–156.

[16] M. Nandi, K. Okada, A. Dutta, A. Bhaumik, J. Maruyama, D. Derks, and H. Uyama, Unprecedented CO_2 uptake over highly porous N-doped activated carbon monoliths prepared by physical activation, *Chem. Commun.*, 2012, **48**, 10283–10285.

[17] M. Sevilla, N. Alam, and R. Mokaya, Enhancement of Hydrogen Storage Capacity of Zeolite-Templated Carbons by Chemical Activation, *J. Phys. Chem. C*, 2010, **114**, 11314–11319.

[18] Z. Yang, Y. Xia, and R. Mokaya, Enhanced Hydrogen Storage Capacity of High Surface Area Zeolite-like Carbon Materials, *J. Am. Chem. Soc.*, 2007, **129**, 1673–1679.

[19] Z. Yang, Y. Xia, X. Sun, and R. Mokaya, Preparation and hydrogen storage properties of zeolite-templated carbon materials nanocast via chemical vapor deposition: effect of the zeolite template and nitrogen doping., *J. Phys. Chem. B*, 2006, **110**, 18424–31.

[20] L. Chen, R. K. Singh, and P. Webley, Synthesis, characterization and hydrogen storage properties of microporous carbons templated by cation exchanged forms of zeolite Y with propylene and butylene as carbon precursors, *Micropor.Mesopor. Mater.*, 2007, **102**, 159–170.

[21] R. Gadiou, S.-E. Saadallah, T. Piquero, P. David, J. Parmentier, and C. Vix-Guterl, The influence of textural properties on the adsorption of hydrogen on ordered nanostructured carbons, *Microporous Mesoporous Mater.*, 2005, **79**, 121–128.

[22] E. Terrés, B. Panella, T. Hayashi, Y. A. Kim, M. Endo, J. M. Dominguez, M. Hirscher, H. Terrones, and M. Terrones, Hydrogen storage in spherical nanoporous carbons, *Chem. Phys. Lett.*, 2005, **403**, 363–366.

[23] M. Oschatz, E. Kockrick, M. Rose, L. Borchardt, N. Klein, I. Senkovska, T. Freudenberg, Y. Korenblit, G. Yushin, and S. Kaskel, A cubic ordered, mesoporous carbide-derived carbon for gas and energy storage applications, *Carbon*, 2010, **48**, 3987–3992.

[24] K. Xia, Q. Gao, C. Wu, S. Song, and M. Ruan, Activation, characterization and hydrogen storage properties of the mesoporous carbon CMK-3, *Carbon,* 2007, **45**, 1989–1996.

[25] Q. Hu, Y. Lu, and G. P. Meisner, Preparation of Nanoporous Carbon Particles and Their Cryogenic Hydrogen Storage Capacities, *J. Phys. Chem. C*, 2008, **112**, 1516–1523.

[26] S. J. Yang, T. Kim, J. H. Im, Y. S. Kim, K. Lee, H. Jung, and C. R. Park, MOF-Derived Hierarchically Porous Carbon with Exceptional Porosity and Hydrogen Storage Capacity, *Chem. Mater.*, 2012, **24**, 464–470.